Taylor & Francis
Taylor & Francis Group

AVIATION
ISSN 1648-7788 print / ISSN 1822-4180 online
2014 Volume 18(1): 44–51
doi:10.3846/16487788.2014.865945

FUNCTIONING OF AN AIR ANTI-COLLISION SYSTEM DURING THE TEST FLIGHT

Jerzy Graffstein

Institute of Aviation, New Technology Centre Department, Warsaw, Poland
E-mail: jgraff@ilot.edu.pl

Received 16 September 2013; accepted 28 February 2014

Jerzy GRAFFSTEIN, *PhD, Eng.*
Education: MSc (Eng.) degree in Aeronautics, Warsaw University of Technology, the Faculty of Power and Aeronautical Engineering. 1999: PhD, Warsaw University of Technology, the Faculty of Power and Aeronautical Engineering, specialization: mechanics.
Affiliations and functions: 1984 to present: researcher, the Institute of Aviation in Warsaw, New Technology Centre Department.
Research interests: modeling of a flying object's motion, automatic flight control along the prescribed trajectory and application of autonomous anti-collision systems in avionics.
Publications: author of 21 scientific articles and co-author of 58 conference papers.

Abstract. The results of research work on an anti-collision system with a radar detector of obstacles, undertaken by the Institute of Aviation, are discussed in the paper. The main tasks set for this system are the detection of static and moving obstacles, estimation of the distance between an aircraft and an obstacle as well as their relative velocity. The functionalities of the system's units and sub-systems are described as well as rules of their cooperation and basic technical parameters which characterise the whole system and its elements. Some in-flight experiments of the anti-collision system are discussed. During these experiments important variables were recorded. The most significant results are analysed and used as the basis for preliminary assessment of the system's operation.

Keywords: anti-collision system, collision avoidance system, avionics.

1. Introduction

The safe realisation of an unmanned aircraft's mission requires a precise plan of the flight trajectory. The most important condition for planning a safe flight is the knowledge about the shape of the terrain where the mission is carried out. Therefore, it is assumed that during the process of the flight trajectory computation a set of known terrain obstacles must be taken into account. However, during a flight some previously unpredicted obstacles: either on ground or moving through the airspace may appear, causing a collision threat to the unmanned object. Anti-collision systems are used in order to detect the previously unknown obstacles and to provide information on evasive manoeuvres. Therefore, in the Institute of Aviation the task to build an anti-collision system which would meet appropriate requirements (described later on) was undertaken. This project was realised, within the framework of development projects, by the Consortium consisting of the Institute of Aviation (coordinator), the Technical University of Warsaw and Microtech International. The aim of the project was to design and construct an autonomous system for the detection of static and moving obstacles: either ground, or airborne. Other important features of this unit include the measurement of the distance between an obstacle and an unmanned air object, the computation of the obstacle's position within Cartesian coordinates and the estimation of the relative velocity of the obstacle. It is expected that software realising the appropriate algorithms (the selected and important elements are presented in (Benayas *et al.* 2002; Graffstein 2012a) will make the system capable of detecting collision threats. The system's functionality was enriched by digital units for the relative altitude measurement and the estimation of climb/

descent velocity, capable of detecting the threat of collision with the ground. Software units were designed to ensure future cooperation between the anti-collision system and the automatic flight control system. The elaborated system project was the base for manufacturing the first tentative unit which was used in ground laboratory tests and first in-flight tests.

2. The structure of the anti–collision system

The general idea of the AURA anti-collision system is presented in the provided diagram (Fig. 1). The system is formed by the following elements: a radar obstacle detector (RDP), a digital radio-altimeter (CRW), an AXMOD RDP micro-computer, an AXMOD CRW micro-computer, the central computer of the anti-collision system, a digital map of the terrain and a database of Obstacles, as well as the reference system AHRS. The system is autonomous and based on three sources of information on obstacles: the Radar Obstacle Detector, the Digital Radio-Altimeter and the Digital Map of the Terrain with the Database of Obstacles. The RDP detects stationary and moving obstacles and estimates their position and velocity (for moving ones). The CRW estimates flight height above the terrain surface as well as the rate of height. Original (primal) signals received from the RDP and the CRW are processed in the AXMOD RDP and the AXMOD CRW micro-computers in order to obtain the appropriate estimates of physical values. The Database of Obstacles contains a set of data (parameters) describing stationary obstacles in the terrain around the desired flight trajectory. The software implemented in the central computer generates the terrain model around the flying object. The software is designed to create and constantly update the database of obstacles including its adequate spatial representation, computed on the basis of data received from the RDP, as well as data representing the motion of the flying object, obtained from the AHRS and the CRW. In each time step, when a new data sequence is acquired from the previously mentioned sources, the risk of a collision with the detected obstacles is estimated. When this condition (Graffstein 2012b) is fulfilled the procedure to find the most appropriate anti-collision manoeuvre is activated. To execute this manoeuvre, an automatic flight control system, which is not a sub–system of the anti-collision system, is necessary.

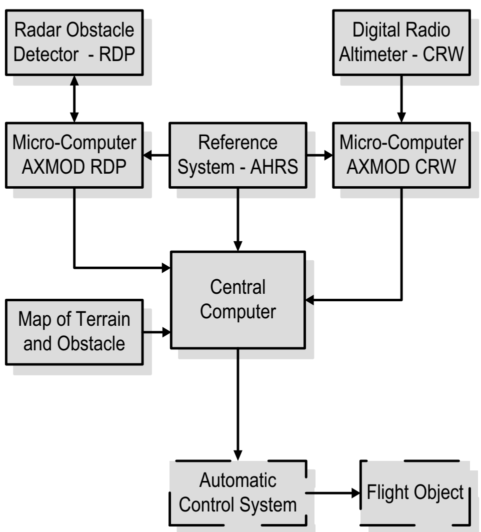

Fig. 1. The general block diagram of the anti-collision system

3. Units of the anti-collision system

The Radar Obstacle Detector is the basic device which delivers information about the current situation within an airspace area surrounding a flying object. It consists of two transmitter/receivers, 24 GHz modules, each one with transmitting and receiving antennas installed on one board of electronic hardware. Both modules are fastened to the upper side of a stiff rotating platform from opposite sides (Fig. 2). The signal is received from the first and second modules interchangeably and then processed successively in the modulator, the washout filter and the amplifier. The transformed signal is transmitted from the rotating platform by a multi-channel rotary joint (with slip rings) to a 16-bit analog-to-digital converter, installed in the lower, immovable part of the RDP's housing. The numerical processing of digits is realised in the AXMOD-RDP computer and The Fast Fourier Transform (FFT) is computed there. Then the obtained spectrum of the signal is analysed to decide on (detect) the existence of hypothetical obstacles within the considered sector. When an obstacle is detected, two characteristic, crucial parameters are determined: the range between the obstacle and the object and the radial velocity of the obstacle towards the object. The RDP is capable of detecting up to five obstacles in one sector with the previously mentioned parameters. Detection is accomplished in a horizontal plane within the front part of a half – sphere, in the section defined by an angle of 156°. This section represents 13 sectors, each one characterised by the angle of 12°. The angular rate of the platform's rotational motion is stabilised at a constant level of 19 rd/s. The range of detection is about 200 m. It depends on the size and shape of the obstacle, as well as on the material the obstacle is made of. The housing of the RDP (Fig. 2) is of a cylinder shape of 170 mm in diameter and 150 mm in height. The overall mass with the housing and the micro – computer AXMOD-RDP inside does not exceed 1,9 kg. The AHRS and the CRW are additional measuring modules ensuring the correct operation of the system. The Attitude and Heading Reference System (AHRS) of type IG-500N, tendered by the SBG Systems company (IG-500N GPS … 2009), is capable of estimating the attitude and linear position of an object flying within a wide range of the airspace. The device also delivers three components: the linear velocity, the angular rate, as well as the components of acceleration. The maximum frequency of sampling used in the AHRS is 100 Hz. The embedded GPS receiver is used to estimate the position in geographical coordinates with a 4Hz frequency (IG-500N GPS … 2009) and the absolute height corrected by pressure sensors. Information, obtained from the AHRS, on the attitude, position, and linear velocity of the flying object is used to compute the estimates of the absolute position and the velocity of the detected obstacle. For example, for the measurment of constant attitude angles, the accuracy is not worse than ±1°. The obtained accuracy of measurements permits classifying this system as being one in the medium class of similar devices. Small dimensions (36×49×22 mm) and a small mass (46 g without a GPS antenna) foreground the advantage of the discussed device. The digital radio - altimeter (CRW, Fig. 3), designed and manufactured in the Institute of Aviation, is capable of measuring the flight height over the surface of the Earth within the range from 0 m to 300 m with a 20 Hz frequency. The obtained accuracy is ±1 m within the range from 0 m to 20 m, and is not worse than about ±5% over this range. The vertical velocity is estimated within the range of ±1 m/s to ±30 m/s. The CRW is a more trustworthy source of information about the relative flight height, when compared with the AHRS. This is why the role of the CRW is important in case of the possibility to use a data base of terrain height. The correlation of the relative flight height and tendencies of it's variation make it capable of forecasting the threat of the crash of the flying object. The apparatus, with the antennas and the AXMOD-CRW micro-computer, is encapsulated within the housing of the dimensions of 204×91×55 mm, and it's overall mass is less than 1.1 kg. The database of the terrain shape is built of text files (tendered by the Geosystem company) containing information on the terrain height and including ground objects. The data was prepared in an orthogonal reference system with a 20×20 m resolution (Jankowski *et al.* 2012).

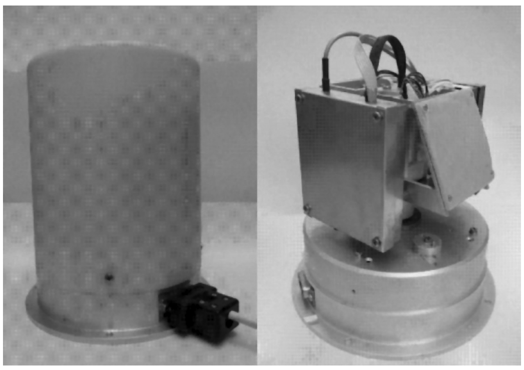

Fig. 2. Radar obstacle detector (RDP)

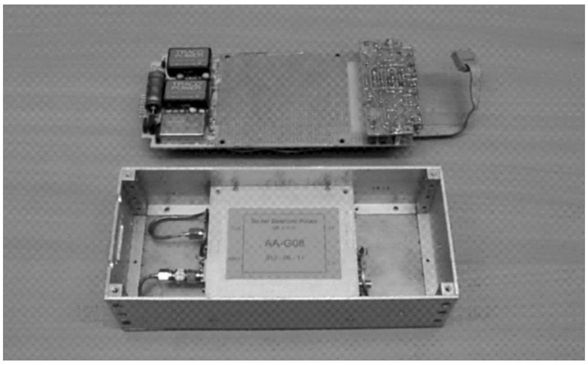

Fig. 3. Elements of Digital Radio Altimeter (CRW)

4. Numerical operations run in the anti-collision system and the method for error computation

All of the necessary computations for the detection of an obstacle and assessment of its characteristic parameters are completed by the anti-collision system. Additionally, approximation of errors for these estimates is possible on the basis of measurements obtained by the same system. The part of measurement results which is used as reference values is obtained in virtue of the specific functionalities of the AHRS unit. In order to obtain the results presented in the paper the following mathematical operations were necessary.

1. The FFT spectrum analysis for subsequent RDP sectors and the computation of the distance to a detected obstacle on the basis of the dominant fringes of this spectrum (Ariyur *et al.* 2005).
2. Computation of the current position of the object in terrestrial coordinates.
3. Transformation of the object and obstacle's positions to the local Cartesian coordinate reference system, fixed on the surface of the Earth with the origin in the flight starting point.
4. Computation of the object-to-obstacle reference distance according to the positions of the object and obstacle (from the AHRS).
5. Computation of the object-to-obstacle distance error as the difference between the results obtained in points 1 and 4.
6. Determination of the obstacle's position in the Cartesian reference system on the basis of the position and attitude in the airspace of the sector where the system detected the obstacle.
7. Analysis of the distribution of dominant fringes in the FFT spectrum of the RDP signal and computation of the relative velocity of the obstacle on this basis.
8. Computation of the relative velocity of obstacle on the basis of the components of object velocity (form the AHRS) and its attitude in the airspace.
9. Computation of the relative velocity error on the basis of the results obtained in points 7 and 8.

10. Mathematical operations described above cover the basic tasks of the anti-collision system. Additional tasks require some computations for assessing the risk of a collision. To do this, several inequalities, describing angular relationships arising from the so called '*collision triangle*' are used, according to the description presented in (Graffstein 2012b; Lalish *et al.* 2009).

5. In-flight testing of the operation of the anti-ollision system

In-flight testing on board of an aircraft is the final method for verifying the correct operation of any avionic unit in its typical environment. A light, two-seater helicopter was used to complete these tests, and was the source of all time histories of the chosen variables (position and velocity), as well as vibrations of a substantial level observed on board. Such an environment is expected to be typical for the tested system which is required to operate properly in these conditions. The operation (the detection and measurements) of the tested system was monitored during several flights of an A 600 Talon helicopter (photo in figure 6). The system's units were installed onto the platform fastened to the landing gear construction beneath the cabin. The RDP radar is visible in the front part above the radio-altimeter while the AHRS and the power supply units were mounted in the rear part (Fig. 6). The trajectory of one test flight near Krosno is presented on the satellite map background (Fig. 4). This trajectory lies in the vicinity of several previously known objects such as a chimney, a tower and an hangar. The photo in figure 5 presents the view from the helicopter's cabin during one of the flights near an obstacle. The results presented further illustrate flights in the vicinity of a 52 m high chimney of the heat supply station, situated at φ = 49,678883333333°N, λ = 21,784294444444°E in terrestrial coordinates. A part of the flight trajectory towards the chimney is presented in figures 7 and 10 in the Cartesian coordinates of the local reference system fixed on the ground. The star symbol denotes the true (GPS measured) position of the obstacle. The first part of the presented trajectory illustrates a quasi-linear flight. The second phase illustrates a turn: the manoeuvre to avoid the obstacle with the appropriate safety margin, and then a flight towards the point where the following series of measurements during the flight towards the previously mentioned obstacle could be repeated. Geometrical signs drawn on the trajectory mark the positions where the considered obstacle was detected. Similar symbols are used to mark the obstacle's position measured by the system. Graphical illustrations of the test results are prepared using metres as units for distance and degrees –for angles. The first two detections of the chimney were recorded within sector 7.

Fig. 4. Helicopter's trajectory during the flight test

Fig. 5. The view from a helicopter's cabin during one of the flight tests

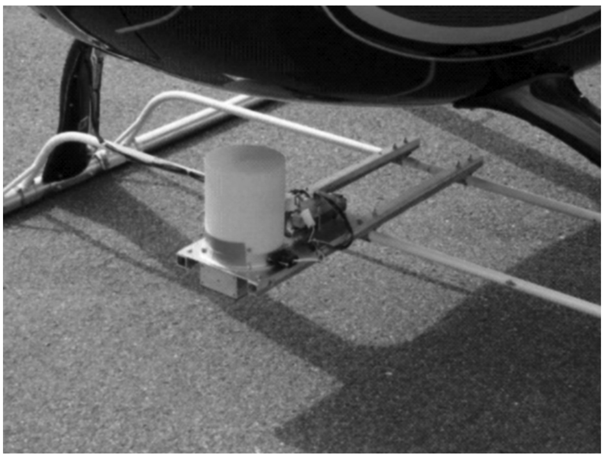

Fig. 6. Installation of the anti-collision system on an A600 "Talon" helicopter

The first one is where the helicopter-to-obstacle distance was close to the maximum range of the RDP radar. These positions were marked in figures 7 and 10 by circles of a diameter adequate to the width of the sector for the considered distance. The last two detections were recorded within sector 6, where the helicopter-to-obstacle distance was about 50 m (Fig. 7). During the flight along the trajectory piece presented in figures 7 and 10 the system continued the measurement and data acquisition process for the necessary physical quantities in order to complete the data about the tested obstacle. To illustrate the system testing conditions, time histories of the following flight parameters are presented in the form of diagrams (Fig. 9): the three angles of the helicopter's attitude: pitch, roll and yaw, the height above the terrain's surface, and the three components of linear ground velocity. Pitch variations in the turn manoeuvre are accompanied by yaw variations. In this phase of motion an increase of the lateral component of velocity, V_y is observed. The resulting velocity of the helicopter's flight along the whole presented part of the trajectory (Fig. 9) is approximately constant, about 30 m/s. The final part of the recorded height measurement is disturbed strongly due to the buildings located in the near vicinity of the heat supply station. In spite of these disturbances, it can be concluded on the base of the time history of this parameter that the flight altitude was kept within the level of about 5–10 m above the upper end of the chimney. Another phase of the helicopter's flight towards the same obstacle was chosen as the example for comparison (Fig. 10). The first detection occured in sector 7, similarly to the previously discussed case, the second and third – in sector 6, and the last one was observed in sector 5. The convention of denoting the points where the obstacle was detected on the trajectory is the same as in the previous example. Similar symbols are used to denote the obstacle's positions computed by the system on the diagram (Fig. 10). The presented example reveals some drawbacks of the system: the first detection of the obstacle appeared several dozen meters closer to the obstacle than the maximum range of the RDP detector. Similarly to the previous cases, the time histories of the helicopter's position variables were recorded for the phase of flight presented in the example (Fig. 10). The disturbance impact on the radio-altimeter measurement was lower than in the case discussed before due to the different shape of the terrain beneath the flight trajectory. In close vicinity of the chimney, the helicopter was moving at approximately 10 m above its top. In the considered phase of flight the helicopter accelerated starting from an initial speed of about 15 m/s up to approximately 35 m/s, as confirmed by the recorded velocity component data (Fig. 12). On the basis of data recorded during this flight, the following system measurement errors concerning the obstacle were estimated: the helicopter -to-obstacle distance, the obstacle's position in the Cartesian coordinates, and the relative speed of the obstacle towards the helicopter. The obtained distance errors were sequenced according to the order of measurements carried out (Fig. 13) and are presented as functions of the helicopter-to-obstacle distance (Fig. 13). The great majority of the performed measurements suffer from errors of less than 10 m, which amounts to 5% of the full range of measurement, 2 of the remaining errors do not exceed 10%, and only one amounts to 12.5%. No correlation was found between these errors and the distance-to-obstacle (Fig. 13).

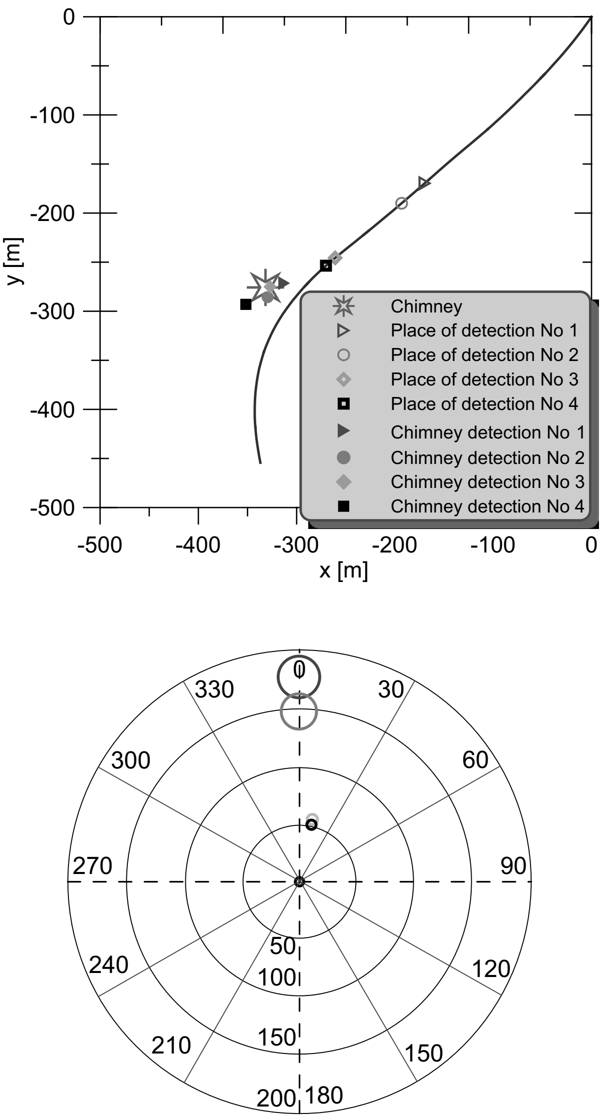

Fig. 7. Place of detection on the trajectory and place of detected chimney

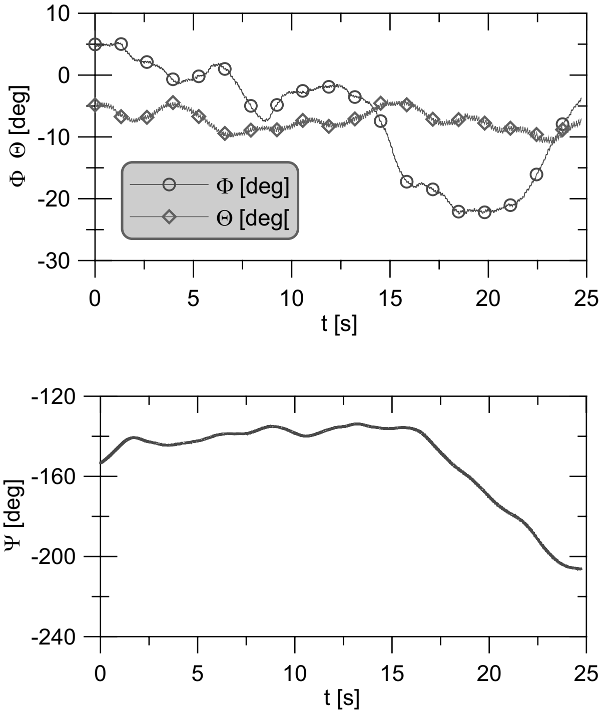

Fig. 8. Time histories of the three angles of the helicopter

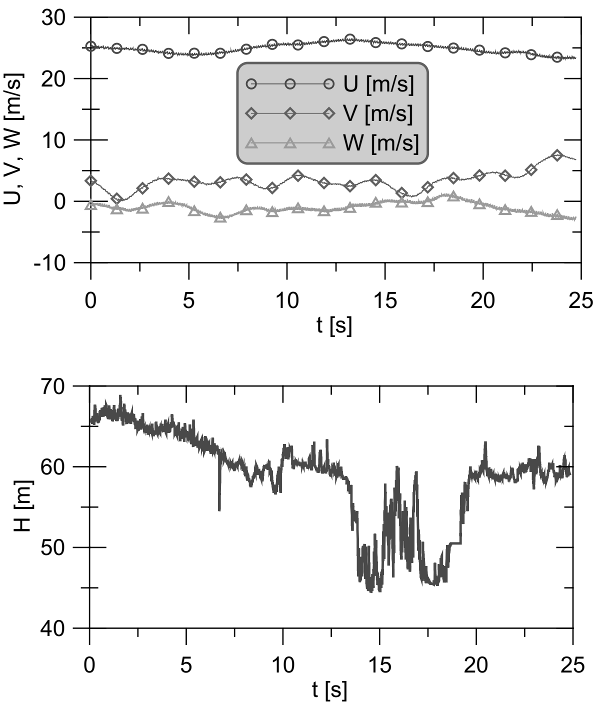

Fig. 9. Time histories of the components of velocity and altitude of the helicopter

The values of the errors regarding the system's estimate of the obstacle's position are presented in the order of the performed measurements (Fig. 14), regarded as a function of distance-to-obstacle (Fig. 14). The method for computing the obstacle's position within the system suffers from errors stemming from several sources. The most relevant of them is the inaccuracy of the RDP measured distance and bias caused by linear resolution. This value depends on the angular width of the radar beam and decreases with the increase of the distance to the obstacle, as indicated by the dotted line in the diagram in figure 14. Another source of this error is the inaccuracy of the GPS based position measurement (within the AHRS reference unit). Taking into account the sum of all errors from these last two sources, the dashed/dotted line, errors of most of the measurements (excluding the two cases mentioned previously) were smaller than this sum. During the flight under discussion a static obstacle was detected, so the assessment of the relative velocity measurement error was easier.

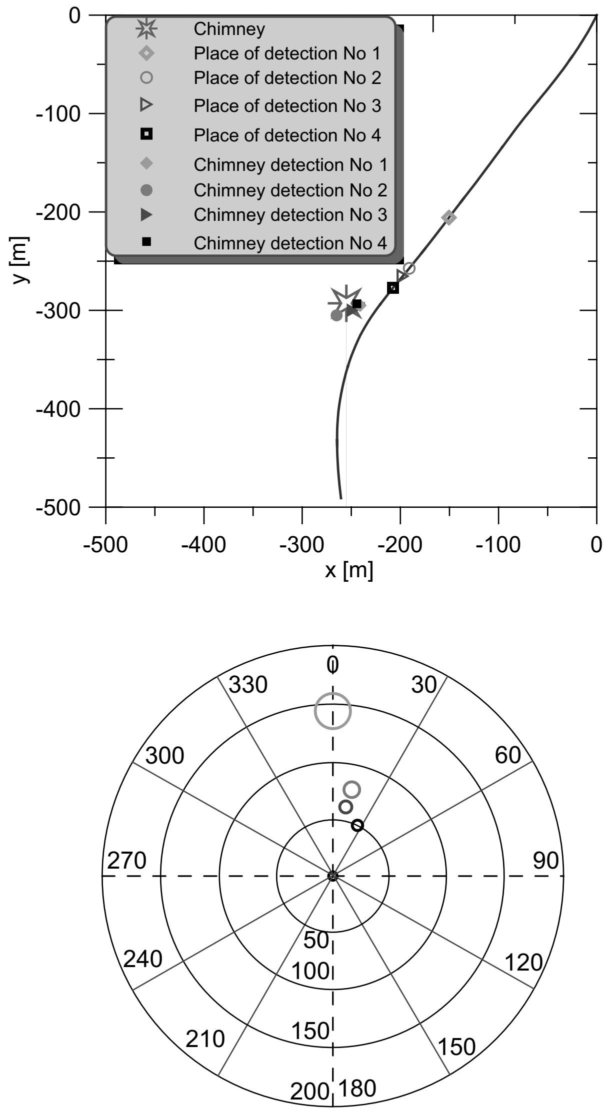

Fig. 10. The place of detection on the trajectory and the place of detected chimney

In this case the system measured the components of the velocity vector of the helicopter's motion (with the signs changed). Quantities of velocity errors are presented, in the order of the measurements taken, in figure 15 as functions of the helicopter-to-obstacle distance. The average error was 3.8 m/s with the maximum value of 8.3 m/s. The AHRS, characterised by a 2 m/s error declared in the horizontal plane, was used as a reference unit for velocity measurement. Taking into account the inaccuracy of this reference unit, the average accuracy of measurement may fluctuate around 1.8 m/s with the maximum value of 6.3 m/s.

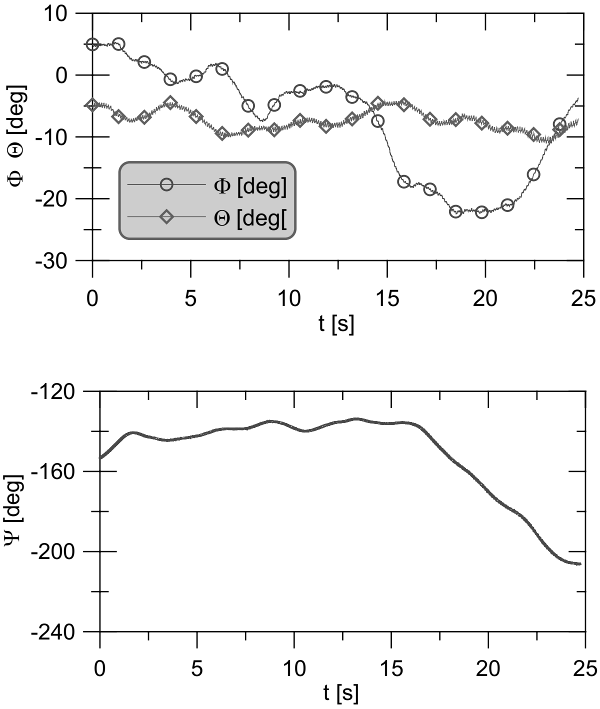

Fig. 11. Time histories of the three angles of the helicopter

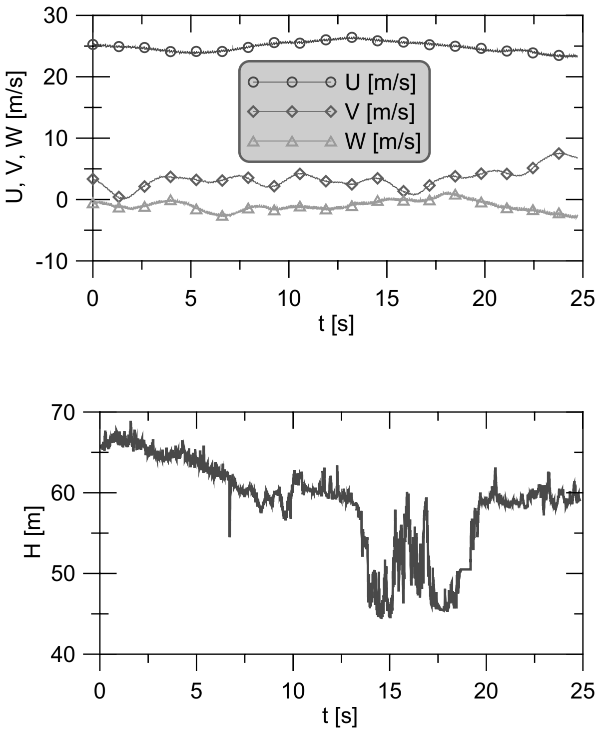

Fig. 12. Time histories of the components of velocity and altitude of the helicopter

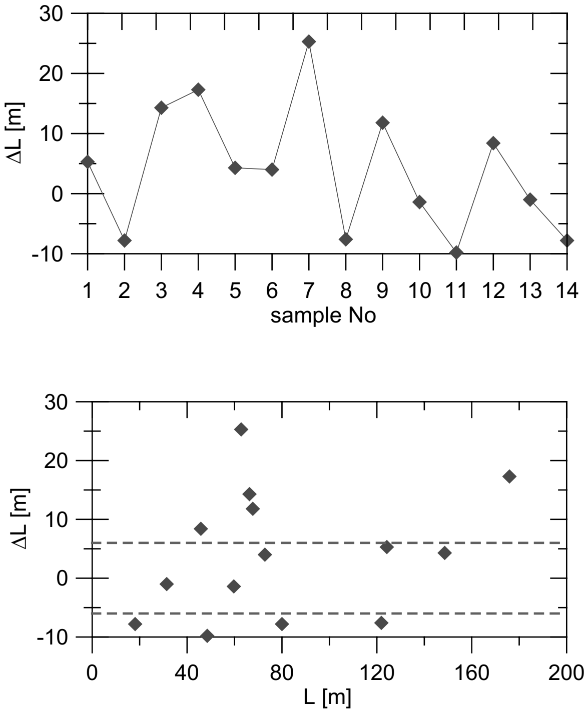

Fig. 13. Error of the distance-to-obstacle

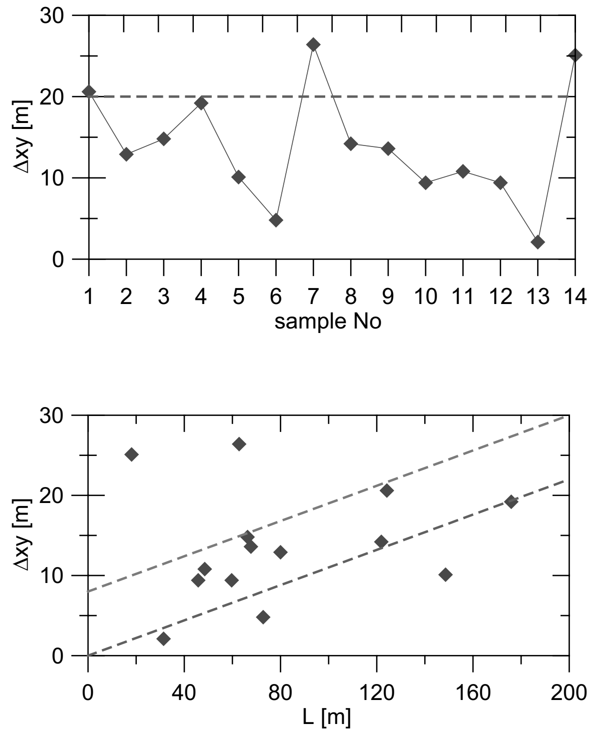

Fig. 14. Error of the obstacle's position

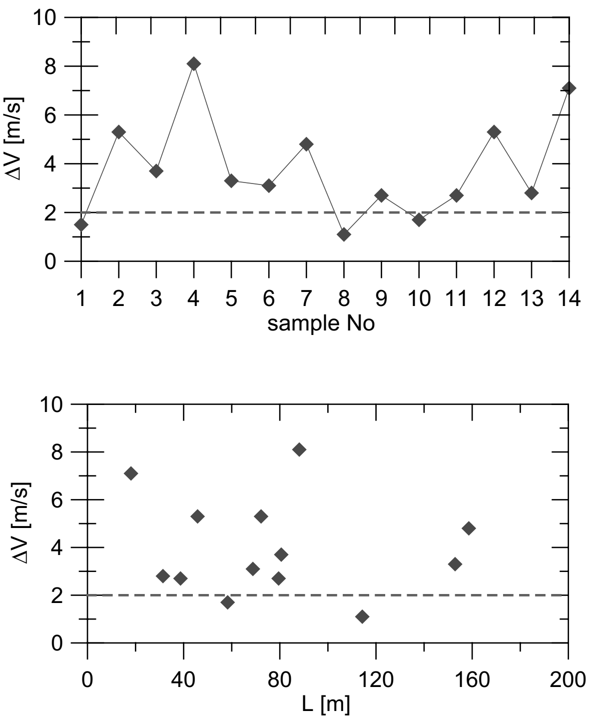

Fig. 15. Error of the obstacle's velocity relative to the helicopter

6. Conclusions

The initial results of the obstacle detection are positive as proven by the analysis of the in-flight test results presented in the paper. The data appears to be a suitable base for tests aimed at detailed verification of the chosen parameters and the introduction of conceivable modifications. The system needs better trustworthiness for the obstacle detection to permit the obstacle detection within the maximum declared distance range. It is expected that higher robustness of the system to disturbances will be necessary for completing this task. One of the necessary conditions for the realisation of the presented ideas is the modification of the system's software based on the results of additional meticulous tests. After some adaptation (mainly of the software part), the system could be used in unmanned automatically controlled flying objects (UAVs) (Koruba, Chatys 2005) as well as in remotely piloted objects or objects piloted with a human crew on board. Objects in the first group need a solution for the question of functionality: sharing between the software of the anti-collision system and the functions realised by the flight control system. Another issue is the distribution of flight control between the anti-collision system and the module responsible for executing the required flight trajectory. The implementation of a graphical interface is necessary in the case of piloted objects. The system described above may be used on objects moving in the airspace at or lower than 300 m with the velocity up to 50 m/s. A more precise estimate of the upper limit of velocity is possible when the object's manoeuvring characteristics are already known.

References

Ariyur, K. B.; Lommel, P.; Enns, D. F. 2005 Reactive in flight obstacle avoidance via radar feedback, in *Proc. of The 2005 American Control Conference*, 8–10 June, 2005, 2978–2982.

Benayas, J. A.; Fernández, J. L.; Sanz, R., *et al.* 2002. The beam-curvature method: a new approach for improving local teal time obstacle avoidance, *The International Federation of Automatic Control* 15(1): 1291. http://dx.doi.org/10.3182/20020721-6-ES-1901.01293

Graffstein, J. 2012a. Anti-collision manoeuvre: process and parameters selection, *Transactions of the Institute of Aviation* (224): 32–45 (in Polish).

Graffstein, J. 2012b. Elements of collision threat detection process and automatically controlled emergency manoeuvres, *Measurements, Automation, Robotics* (2): 383–387.

IG-500N GPS aided AHRS User Manual SBG Systems. 2009.

Jankowski, S.; Szymański, Z.; Szczyrek, J. 2012. Reconstruction of environment model by using radar vector field histograms, in *Proc. of SPIE* 8454 (845422), *Photonics Applications in Astronomy, Communications, Industry, and High-Energy Physics Experiments*, 15 October, 2012, Wilga, Poland.

Koruba, Z.; Chatys, R. 2005. Gyroscope-based control and stabilization of unmanned aerial mini-vehicle (mini-UAV), *Aviation* 9(2): 10–16.

Lalish, E.; Morgansen, K. A.; Tsukamaki, T. 2009. Decentralized reactive collision avoidance for multiple unicycle-type vehicles, in *American Control Conference,* 11–13 June, 2008, *Seattle*, 5055–5061. http://dx.doi.org/10.1109/ACC.2008.4587295